Surface Chemistry Effects on the Reactivity and Properties of Nanoconfined Bisphenol M Dicyanate Ester in Controlled Pore Glass

Qingxiu Li and Sindee L. Simon*

Department of Chemical Engineering, Texas Tech University, Lubbock, Texas 79409

Received December 17, 2008; Revised Manuscript Received April 8, 2009

ABSTRACT: Nanoconfinement has been found to have significant effect on the glass transition behavior of low molecular weight and polymeric glass formers. Here, we investigate the influence of nanoconfinement on the cure kinetics and glass transition temperature of a bisphenol M dicyanate ester/polycyanurate material as a function of surface chemistry and nanoconfinement size in native and silanized controlled pore glasses (CPGs). The glass transition temperature and conversion as a function of cure time are examined using differential scanning calorimetry (DSC). The native CPG surface accelerates the cure of bisphenol M dicyanate to a larger extent compared to the silanized hydrophobic CPG presumably because of the catalytic nature of hydroxyl groups on the CPG wall. Two T_gs are observed for both monomer and polycyanurates confined in the native CPGs. The primary T_g of the "fully cured" polycyanurate is depressed by 60 K at 11.5 nm, and the secondary T_g is 10−33 K above the primary T_g; the values are similar to those found previously in silanized CPGs. The length scale associated with the secondary T_g is ∼0.90 nm assuming that the secondary T_g reflects the material at the CPG wall surface. Based on the measurements of T_g, the total heat capacity change at T_g, and the sol content, all as a function of conversion, the network structure does not change upon nanoconfinement.

Introduction

Nanoconfinement has been found to have a great impact on the glass transition behavior of low molecular weight and polymeric glass formers.[1−9] The glass transition temperature (T_g) is generally depressed upon nanoconfinement; however, increases or no change in T_g have also been observed.[1−9] The nanoconfinement effect on glass transition temperature can be enhanced or weakened by changing side-chain length,[10] addition of diluent,[11] or modification of chain stiffness.[12] For thin films of poly(*n*-alkyl methacrylate) with various alkyl chain lengths, depressions in the coefficient of thermal expansion (CTE) and the T_g of the thin films relative to the bulk increase with decreasing alkyl chain length.[10] This enhancement of the T_g−nanoconfinement effect is attributed to an increase in the size of the cooperatively rearranging region (CRR)[10] following explanations in earlier work.[13] On the other hand, a reduction of the effect of nanoconfinement on T_g is observed for polystyrene films with addition of diluent, such as pyrene or dioctyl phthalate (DOP).[11] The T_g depression decreases with increasing pyrene or DOP concentration, and at 9 wt % of pyrene or 4 wt % of DOP, the T_g of the thin film shows bulk behavior down to 13 nm. The reduction of the effect of nanoconfinement on T_g with the addition of diluent was also ascribed to a decrease in the size of the cooperative segmental dynamics.[11] In addition, Torkelson and co-workers also hypothesized that the effect of nanoconfinement on T_g is enhanced with an increase in chain stiffness.[12] For example, supported thin films of poly(4-*tert*-butylstyrene) (PTBS), with higher chain stiffness, show stronger nanoconfinement effects (i.e., greater T_g depressions at a given film thickness) compared to poly(4-methylstyrene) (P4MS) and polystyrene (PS). Similarly, polycarbonate (PC) thin films exhibit an enhanced effect of nanoconfinement on T_g when compared to polystyrene presumably due to its significantly greater chain stiffness.[14] For our previous work on bisphenol M dicyanate ester (BMDC) confined in silanized (hydrophobic) controlled pore glasses (CPGs), the effect of nanoconfinement on T_g also increases upon polymerization.[15] Whether the changes in the nanoconfinement effect on T_g as a function of conversion in thermosetting polymers is caused by changes in the cooperativity length scale, chain stiffness, or both requires clarification.

Despite the extensive research on the effect of nanoconfinement on the glass transition of small molecule and thermoplastic glass formers,[1−9] the work on thermosetting materials is extremely limited. Wang and Zhou studied the glass transition temperature of the microtome-sliced epoxy thin film.[16] The T_g was found to decrease with film thickness, and a T_g depression of 15 K was observed for a 40 nm thin film.[16] Recently, we have found that nanoconfinement increases the rate of the cure kinetics of a bisphenol M dicyanate ester thermosetting resin cured under the well-defined nanoscale constraint of hydrophobic silanized controlled pore glasses.[15] In that work, T_g depressions were also observed for both the bisphenol M dicyanate ester monomer and the polycyanurate networks; the magnitude of the T_g depression was more pronounced for the "fully cured" network compared to the monomer.

Our previous study excluded the influence of pore surface chemistry on the cure kinetics and glass transition of thermosetting resin since only silanized controlled pore glasses were used in which the hydroxyl groups on the pore surface were replaced by the trimethylsilyl groups.[15] Surface interactions can influence the glass transition behavior and, moreover, could influence reaction rates. In fact, it is known the cure reaction of cyanate esters can be catalyzed by the hydroxyl groups.[17] Consequently, the purpose of this study is to investigate the effects of pore surface chemistry and pore size on the cure kinetics and glass transition of bisphenol M dicyanate ester confined in the nanopores of controlled pore glasses. Specifically we examine the behavior in native hydrophilic nanopores in this work and compare the T_g depression and cure kinetics to those found previously[15] for silanized CPGs. The influence of conversion on the T_g depression is also examined. We also investigate the influence of nanoconfinement on the sol content vs conversion relationship using silanized CPGs.

Experimental Section

Materials. The thermosetting resin used is bisphenol M dicyanate ester (BMDC, trade name RTX-84921 from Hi-Tek Polymers,

* Corresponding author: e-mail sindee.simon@ttu.edu.

10.1021/ma802808v CCC: $40.75
Published on Web 04/27/2009

Table 1. Specifications of Controlled Pore Glasses

product name	mean pore diameter (nm)[a]	pore diameter distribution (%)[b]	specific pore volume (cm^3/g)[a]	specific surface area (m^2/g)[c]
CPG00120B	11.5	7.3	0.49	119.5
CPG00240B	24.6	7.7	0.83	79.6
CPG500A	50.0	3.7	1.10	50.9
CPG01000B	110.6	3.6	1.06	25.0
CPG1400B	122.1	3.7	1.73	31.2
CPG3000B	287.8	5.3	1.06	8.6

[a] Determined by the mercury intrusion method. [b] Analyzed by the ultrasonic sieving method. [c] Measured by the nitrogen adsorption method.

Louisville, KY) in the solid form. The cure reaction of this monomer and the resulting physical and viscoelastic properties have been previously studied in bulk[17,18] and under the nanoconfinement of silanized hydrophobic CPGs.[15]

The confinement mediums are native controlled pore glasses (CPGs) with pore size ranging from 11.5 to 287.8 nm, purchased from Millipore (Billerica, MA). The specifications of the CPGs are tabulated in Table 1 as provided by the manufacturer. Prior to the imbibition of the resin in the nanopores, the CPGs were cleaned by immersing in 69.7% nitric acid at around 100 °C for 10 h, rinsed well with distilled water, and dried at 285 °C in a vacuum oven for 24 h. The cleaned CPGs were kept in a desiccator to eliminate moisture absorption. For the sol extraction experiments described later, the CPGs with pore sizes of 50.0 and 122.1 nm were further silanized using hexamethyldisilazane, as in our prior work,[15] to convert the surface hydroxyl groups into trimethylsilyl groups.[19]

The borosilicate CPG is expected to be insoluble in the BMDC resin and the resulting polycyanurate network. Backing up this assertion that nonpolar liquids do not leach material out of the CPG, the melting point depression of benzene in 8.1 nm CPG nanopores was measured 10 min after initial imbibement and as a function of time after imbibement for times up to 1 week. The melting point depression was found to be constant at 14.79 ± 0.05 K in native 8.1 nm pores, independent of time in the pores for times from 10 min up to 1 week; similarly for hydrophobic 8.1 nm pores that had been silanized with hexamethyldisilazane, the melting point depression was constant at 16.10 ± 0.03 K over the course of 1 week. For these experiments the change in melting point was measured in slightly overfilled pores by the difference in the onset of melting between material in the pores and the bulk material external to the pores. The results indicate that the CPG nanopores are a stable matrix for nanoconfinement of nonpolar liquids and glasses.

Samples for differential scanning calorimetry (DSC) were made by placing a specified mass of BMDC monomer on top of a known mass of CPG in a DSC pan; the pan was then held at 100 °C for 3 min to allow melting of the crystalline monomer and imbibition into the CPG. The fullness of the pores was controlled from 95% to 100% based on the weight of the monomer added and its density (1.14 g cm^{-3}) relative to the CPG pore volume (Table 1). We emphasize that the resin is imbibed in the nanopores of the CPGs, such that the sample is one of the resin or polymer confined in the CPG nanopores; it is not a traditional composite in the sense that there should be no significant amount of polymer matrix surrounding (or outside of) the CPG particles.

The imbibition velocities of BMDC monomer in the native CPGs were calculated following Huber's equation[20] with all the parameters reported in the previous paper,[15] except that the contact angle of BMDC on the native borosilicate glass at room temperature is smaller: 42 ± 1° as measured on a Ramé-Hart goniometer; the resulting imbibition time for BMDC is less than 2 s in the largest native pores and is less than 6 min in the smallest pores. Samples used in the isothermal cure study were further held at 100 °C for 10 h to ensure complete imbibition in the pores—this length of time was chosen prior to publication of Huber's paper.

DSC Measurements. The DSC measurements were performed on a Mettler Toledo differential scanning calorimeter DSC823e with a Julabo FT100 intracooler and nitrogen purge gas. Measurements of the glass transition temperature of the confined unreacted monomer (T_{go}), the total heat of reaction (ΔH_T), and the onset of the reaction exotherm (T_{onset}) were measured on heating at 10 K/min after imbibement at 100 °C for 3 min; the error bars reported for these values are based on the standard deviation of three different samples for ΔH_T and T_{onset} and based on nine samples for T_{go}. The glass transition temperature and conversion (x) were also studied as a function of cure time for isothermal cure at 180 °C; in these studies after curing for a specified time from 0 to 192 h, the sample was cooled at 10 K/min to −60 °C, and then T_g and conversion were measured on heating at 10 K/min to 380 °C. Error bars reported for isothermal cure data points are the standard deviation for a minimum of two runs performed at the same cure condition. It is also noted that isothermal cure studies were performed after imbibition in the native CPGs at 100 °C for 10 h. Hence, the total conversions at the start of cure at 180 °C is estimated to range from 0.7% to 9.6% for the monomer in the CPGs with pore sizes of 287.8 to 11.5 nm; this initial conversion is corrected for in the kinetic analysis.

The glass transition temperature was determined on the heating scan by measuring the limiting fictive temperature (T_f') based on the method of Moynihan:[21]

$$\int_{T_f'}^{T>T_g} (C_{pl} - C_{pg})\, dT = \int_{T<T_g}^{T>T_g} (C_p - C_{pg})\, dT \qquad (1)$$

where C_{pg} and C_{pl} represent the temperature-dependent glassy and liquid heat capacities, respectively. The limiting fictive temperature T_f' measured on heating after cooling at a given rate is approximately equal to T_g measured on cooling at the same rate;[22] consequently, we use T_g for the sake of simplicity in the rest of the article.

The conversion (x) was determined from the residual heat of reaction (ΔH_r) according to the following equation:[15]

$$x = \frac{\Delta H_T - \Delta H_r}{\Delta H_T} \qquad (2)$$

where ΔH_T is the total heat of reaction of an initially uncured sample.

The Mettler Toledo DSC was also used to measure the absolute heat capacity of bisphenol M dicyanate ester monomer and polycyanurate in the bulk state by applying the TOPEM program. TOPEM was run using a heating rate of 2 K/min, pulse height of 0.25 K, and pulse time of 15−30 s for the scan temperature range from T_g − 65 °C to T_g + 35 °C. The resulting absolute heat capacity was used to calculate the length scale of the monomer and polymer at glass transition temperature, ξ, based on the Donth's model:[23]

$$\xi^3 = k_B T^2 \Delta(1/C_v)/(\rho \delta T^2) \qquad (3)$$

where k_B is the Boltzmann constant, $\Delta(1/C_v)$ is the step change in the reciprocal of the specific heat of the glass and the liquid at constant volume, ρ is the density of the sample, and δT is the temperature fluctuation of one average CRR at temperature T. The term $\Delta(1/C_v)$ is taken to be $0.74\Delta(1/C_p)$, where $\Delta(1/C_p)$ is the reciprocal of the isobaric heat capacity change at T_g.[23] The term δT is estimated to be $\delta T = \Delta T/2.5$, where ΔT is the temperature interval where the $C_p(T)$ varies between 16% and 84% of the ΔC_p step on a heating scan.[23]

The temperature of the DSC was calibrated with mercury and indium at 10 K/min on heating and was maintained at an accuracy of 0.1 °C for the glass transition temperature and heat of reaction measurements. For the absolute heat capacity measurement, the temperature calibration of DSC was performed using mercury, indium, and tin at 0.1 K/min on heating, which is equivalent to isothermal calibration as suggested in previous work.[24] Sapphire was used as the calibration substance for heat capacity. The heat flow of DSC was calibrated using indium for both types of measurements.

Sol Extraction. Sol extraction was performed to determine the gel point of bisphenol M dicyanate ester cured under the nanoconfinement of silanized CPGs with pore diameters of 50.0 and 122.1

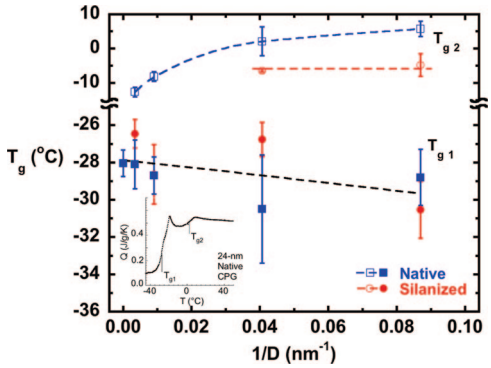

Figure 1. T_g as a function of reciprocal pore diameter for bisphenol M dicyanate ester monomer confined in native and silanized CPGs as well as in the bulk state. The inset shows a typical DSC heating scan displaying two T_gs for resin confined in 24.6 nm native pores. Data for silanized CPGs are from ref 15. Error bars are the standard deviation based on at least nine samples.

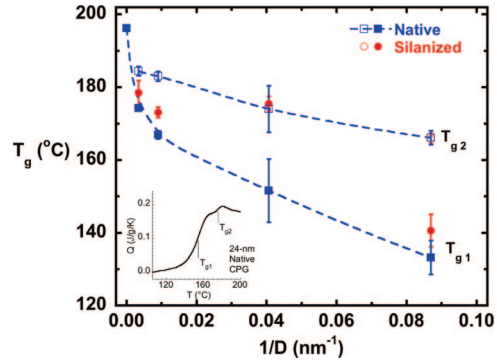

Figure 2. T_g as a function of reciprocal pore diameter for fully cured polycyanurate confined in native and silanized CPGs as well as in the bulk state. The inset shows a typical DSC heating scan displaying two T_gs for the polycyanurate confined in 24.6 nm native pores. Data for silanized CPGs are from ref 15. Error bars are the standard deviation based on at least three samples.

nm. BMDC monomer was first imbibed in the CPGs at 100 °C for 10 h under a nitrogen atmosphere with fullness ranging from 95% to 100%. The monomer was subsequently cured at 180 °C for various times ranging from 1 to 120 h under vacuum. The partially cured sample under nanoconfinement was immersed in tetrahydrofuran for 7 days at room temperature to extract the sol. Upon removal of the sol, the remaining gel in the pores was first air-dried for 12 h at room temperature; the residual solvent was further removed under vacuum at room temperature for 24 h and 150 °C for 48 h. The sol content was determined based on the sample weight before and after sol extraction; initial sample weights (resin plus CPG) ranged from 90 to 235 mg, whereas final sample weights ranged from 45 to 165 mg.

Results

***T_g* of Bisphenol M Dicyanate Ester Monomer.** The glass transition temperature of bisphenol M dicyanate ester monomer confined in the native CPGs is shown in Figure 1; also shown is the dependence of T_g on pore size for silanized CPGs from ref 15. Two T_gs are observed in all of the native pores. The inset in the figure shows a typical DSC heating scan displaying these two T_gs for resin confined in the 24.6 nm pores. On the other hand, the secondary (upper) T_g is only observed in the smallest 11.5 and 24.6 nm silanized pores. The primary (lower) T_g shows a weak dependence on the pore diameter, and it decreases with decreasing pore diameter for both surface chemistries. The secondary (upper) T_g increases with decreasing pore diameter and is higher in the native CPGs. The secondary (upper) T_g in the silanized CPGs at 11.5 and 24.6 nm was attributed to the physical trapping of the monomer in the rough surface of the silanized CPGs.[15] For the native CPGs, in addition to physical trapping, strong interactions resulting from hydrogen bonding between the monomer and the hydroxyl groups on the surface of the CPGs may contribute to the higher secondary T_g.

***T_g* of "Fully Cured" Polycyanurate Networks.** The glass transition temperature of the "fully cured" polycyanurate networks confined in the native and silanized CPGs, the latter from ref 15, with various pore diameters is shown in Figure 2. Two T_gs are observed for all of the native pores. The inset in the figure shows a typical DSC trace showing these two T_gs for the polycyanurate confined in the 24.6 nm porse. On the other hand, two T_gs are observed only for the smallest silanized pores. The primary T_g is depressed by 60 K at 11.5 nm in the native pores; the secondary T_g is 10−33 K above the primary T_g, yet still below the bulk value. Both primary and secondary T_gs decrease monotonically with decreasing pore diameter in the native pores, which differs from the behavior of the primary T_g in the silanized pores, where a nonmonotonic decrease of T_g with decreasing pore size is observed. The values of the secondary (upper) T_gs in both native and silanized CPGs are comparable, indicating that the hydrogen-bonding contribution becomes weaker upon the formation of networks; this is consistent with the decrease in polarity of the resin as the cyanate groups react to form triazine.

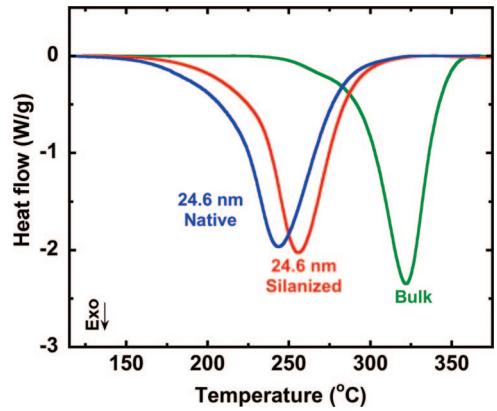

Figure 3. Ramp cure of bisphenol M dicyanate ester at 10 K/min up to 380 °C in the bulk state (green) and confined in the native (blue) and silanized (red) CPGs of 24.6 nm after imbibition at 100 °C for 3 min.

Ramp Cure of Bisphenol M Dicyanate Ester. Ramp cure of bisphenol M dicyanate ester at 10 K/min for the bulk state is compared to that for the resin confined in 24.6 nm native and silanized CPGs in Figure 3. The total heat of reaction and the exotherm onset temperature for the bulk resin and as a function of pore diameter for the native and silanized CPGs are listed in Table 2. The total heat of reaction does not vary with pore size, and the value is comparable with that in the bulk state, indicating that the cure reaction under nanoconfinement goes to completion. The onset temperature decreases significantly with pore size, indicating that nanoconfinement accelerates the cure of BMDC monomer. In addition, the onset temperature is lower in the native CPGs than in the silanized pores, indicating that the native surface promotes the reaction.

Isothermal Cure Kinetics of Bisphenol M Dicyanate Ester. As shown in Figures 1 and 2, the primary T_g of the resin increases from its uncured value near −28 °C to a bulk fully cured value of 196 °C or, under nanoconfinement, to a depressed, but fully cured, value of around 135 °C at 11.5 nm. The large changes of T_g that accompany cure of thermosetting

Table 2. Total Heat of Reaction and Onset Temperature of the Monomer under Nanoscale Constraints of Native and Silanized CPGs at Different Pore Sizes[a]

mean pore diameter (nm)		∞ (bulk)	287.8	110.6	24.6	11.5
ΔH (kJ/mol OCN)	native	110.0 ± 7.8	114.6 ± 1.5	113.4 ± 2.9	114.7 ± 0.6	108.7 ± 6.1
	silanized		111.9 ± 1.2	111.4 ± 3.3	111.6 ± 2.9	113.2 ± 6.1
T_{onset} (°C)	native	292.2 ± 1.0	247.8 ± 0.6	239.7 ± 8.9	211.4 ± 2.5	215.8 ± 1.3
	silanized		247.3 ± 7.4	242.4 ± 2.3	217.3 ± 9.6	206.7 ± 20.3

[a] Values reported are the average ± standard deviations based on three individual measurements.

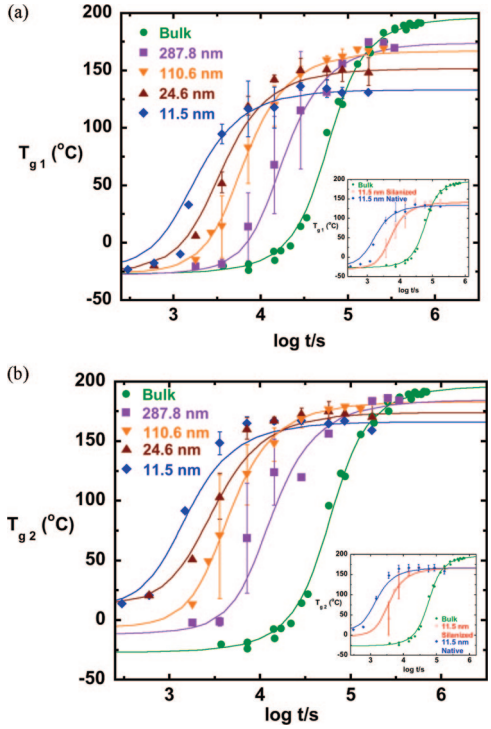

Figure 4. (a) The primary T_g, T_{g1}, and (b) the secondary T_g, T_{g2}, as a function of cure time in the bulk state and confined in the native CPGs. The inset shows the comparison between material cured in 11.5 nm native CPGs (blue solid symbols) and in 11.5 nm silanized CPGs (red open symbols from ref 15). The solid lines are the fits to the kinetic equation (eq 4).

resins even under nanoconfinement, coupled with the unique relationship between T_g and conversion (see later), allow us to use the T_g changes to monitor the reaction. Figure 4a,b shows the evolution of the primary and secondary T_gs as a function of cure time at 180 °C for bisphenol M dicyanate ester confined in the native CPGs. The bulk behavior is also shown, and the insets also compare T_g as a function of cure time in the silanized and native CPGs at 11.5 nm and in the bulk state. The solid lines are fits to a second-order plus second-order autocatalytic cure kinetic equation:[17]

$$\frac{dx}{dt} = k\alpha(1 - x)^2(x + b) \tag{4}$$

where x is conversion, t is cure time, k and kb are the Arrhenius rate constants for the second-order autocatalytic and second-order reactions, respectively, and α is the acceleration factor. The kinetic equation describes the data well. Note that the initial conversion after the 10 h hold at 100 °C as described in the Experimental Section was taken into account in the fitting. In the native CPGs, the cure rate increases as pore size decreases, and consistent with the ramp cures shown in Figure 3, the cure reaction in the native CPGs is faster than that in the silanized ones at a given pore size.

The acceleration factor α determined based on the kinetic fit to the isothermal cure data shown in Figure 4 is shown in Figure 5 as a function of reciprocal pore size for both native and

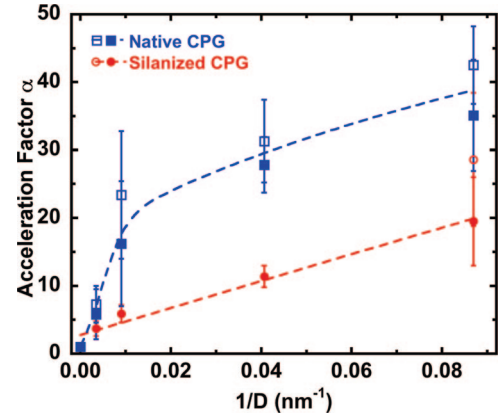

Figure 5. Acceleration factor as a function of reciprocal pore diameter for native and silanized CPGs. The solid symbols represent the primary T_g (T_{g1}), and the open symbols represent the secondary T_g (T_{g2}). The standard deviation of acceleration factor was determined by fitting the lower and upper bound of the cure data, i.e., the T_g as a function of cure time shown in Figure 4. The dashed lines are intended only as a guide to the eye. Acceleration factors for material in silanized pores are recalculated from the kinetic data in ref 15.

silanized pores. The acceleration factor is a strong function of pore size, increasing with decreasing pore size. The acceleration factor is also dependent on surface chemistry, with cure being accelerated in the native CPGs and even faster for T_{g2}. An acceleration factor of 35 is obtained for T_{g1}, and a value of 43 is obtained for T_{g2} in the 11.5 nm native CPG, whereas values of 20 and 29, respectively, are obtained for cure in the silanized pores. We note that the acceleration factors for the silanized CPGs reported in our previous work[15] were mistakenly calculated due to an algebraic error; the correct values are reported here and shown in Figure 5. The enhanced reaction rates in the silanized CPGs were attributed, in our prior work,[15] to the increased collision efficiency due to the decreased mobility (i.e., decreased degrees of freedom) of the molecules in the surface layer. For the native pores, the additional acceleration is presumably due to catalysis by the hydroxyl groups on the CPG wall; the fact that triazine also accelerates the reaction (i.e., the reaction is autocatalytic) may account for the enhanced acceleration in the native pores away from the wall.

Relative T_g vs Conversion. As previously alluded to, the glass transition temperature is a unique function of conversion for cyanate ester/polycyanurate thermosets,[17] and this relationship is plotted in Figure 6 along with those from the bulk and silanized CPGs. The normalized T_g is plotted:[25]

$$T_g^* = \frac{T_g - T_{g,0}}{T_{g,\infty} - T_{g,0}} \tag{5}$$

Since we observed two T_gs in the native CPGs, the T_g value used is the average glass transition temperature $T_{g,avg}$ determined based on the primary T_g (T_{g1}) and secondary T_g (T_{g2}) and weighted by their corresponding heat capacity changes at T_g, $\Delta C_{p,1}$and $\Delta C_{p,2}$:

$$T_{g,avg} = \frac{T_{g1}\Delta C_{p,1} + T_{g2}\Delta C_{p,2}}{\Delta C_{p,1} + \Delta C_{p,2}} \quad (6)$$

This weighting is in essence a weighting by mass fraction assuming that the masses of material participating in the primary and secondary T_gs are proportional to the respective step changes in heat capacity.

All of the data, including for the bulk and for the material confined in the native and silanized CPGs, collapses onto a single curve which can be described by the DiBenedetto equation:[25]

$$T_g^* = \frac{\lambda x_T}{1 - (1 - \lambda)x_T} \quad (7)$$

where x_T is the total conversion and λ is the structural fitting parameter.[17] The fitting yields a single λ at 0.423 ± 0.016, indicating that the network structure does not change under nanoconfinement. The value of λ has been proposed by Pascault and Williams[26] to be theoretically related to the step changes in the heat capacity for the uncured and fully cured resin, ΔC_{p0} and $\Delta C_{p\infty}$, respectively:

$$\lambda = \frac{\Delta C_{p\infty}}{\Delta C_{p0}} \quad (8)$$

The relationship between ΔC_p and conversion is shown in Figure 7 to be independent of pore size within the scatter of the data. Experimentally, we find $\Delta C_{p0} = 0.50 \pm 0.07$ J g^{-1} K^{-1} at $x =$ 0 (based on nine samples) and $\Delta C_{p\infty} = 0.22 \pm 0.04$ J g^{-1} K^{-1} at $x = 1$ (based on three samples). Thus, we obtain a value of $\Delta C_{p0}/\Delta C_{p\infty} = 0.44$, consistent with the value of λ obtained from the DiBenedetto equation.

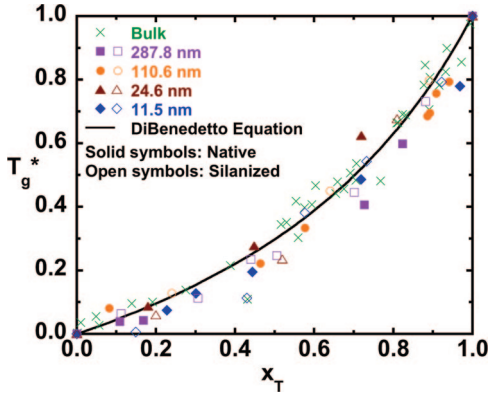

Figure 6. Relative T_g (as defined in eqs 5 and 6) as a function of conversion of bisphenol M dicyanate ester cured in the bulk and confined in the native and silanized CPGs. The solid line is the fit to the DiBenedetto equation (eq 7). Data for silanized CPGs are from ref 15; bulk data are from ref 17.

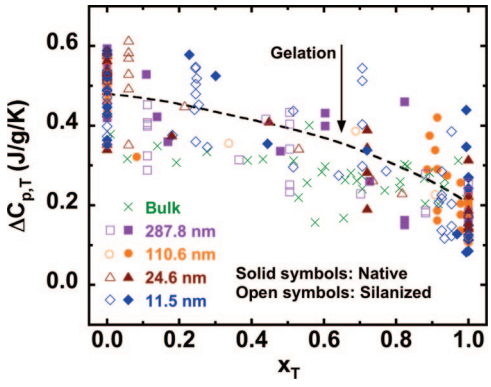

Figure 7. Total heat capacity change at T_g as a function of total conversion for bisphenol M dicyanate ester cured in the bulk state and confined in the native and silanized CPGs of various sizes. The bulk data are augmented by unpublished data of Simon and Gillham.[41] The dashed line is intended only as a guide to the eye.

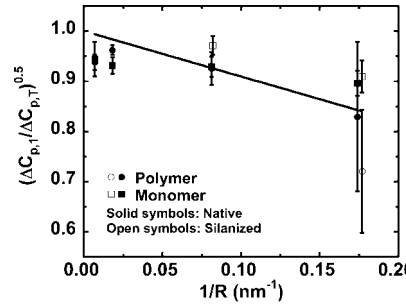

Figure 8. Square root of the fractional heat capacity change at T_{g1} vs reciprocal pore radius ($R = D/2$). The fit results in a length scale of 0.90 ± 0.15 nm for the presumed surface layer associated with the secondary T_g. Error bars are the standard deviation of the quantity $(\Delta C_{p,1}/\Delta C_{p,\text{total}})^{1/2}$ based on a minimum of nine samples for the monomer and at least three samples for the polymer.

Discussion

Length Scale Associated with the Secondary T_g. Nanoconfinement of glass formers often results in a secondary T_g or relaxation observed at temperatures above the primary T_g. The strength of the secondary T_g increases at smaller confinement size,[9,27−39] and the relaxation has been attributed to a less mobile layer formed in the vicinity of the confining medium surface due to the physical or chemical trapping (i.e., a two-layer model).[28,31] For glass formers confined in controlled pore glasses, the thickness of this surface layer can be determined based on the heat capacity change at T_g associated with the two glass transitions following Equation 9 assuming cylindrical pores and that the density of the glass former does not change along the pore radius:[15,27]

$$\sqrt{\frac{\Delta C_{p,1}}{\Delta C_{p,T}}} = 1 - \frac{L}{R} \quad (9)$$

where $\Delta C_{p,1}$ is the heat capacity change associated with T_{g1} and $\Delta C_{p,T}$ is the total heat capacity change at T_g; L is the length scale of the surface layer; and R is the pore radius. The length scale L can be determined from a plot of the square root of the fractional heat capacity change at T_{g1} vs reciprocal pore size. The fit is shown as the solid line in Figure 8 for both monomer and "fully cured" polymer in the native and silanized CPGs. The resulting thickness of the surface layer is 0.90 ± 0.15 nm, which is consistent with the cooperative length scale associated with T_g.

We note that if the inverse assumption were made, that the primary T_g is associated with the interfacial material near the wall and the secondary T_g is associated with the material in the center of the pore, then $(\Delta C_{p2}/\Delta C_{p\text{Total}})^{1/2}$ vs $1/R$ should be show a linear relationship with a y-intercept of 1.0 and a slope being equal to the negative of the interface thickness. However, such a plot displays a y-intercept of 0.3 and a positive slope—indicating either that this interpretation is wrong or that the interface thickness depends strongly on pore size. We suggest that the former is more likely given that the data are consistent with the assumption of a constant interfacial thickness when the secondary T_g is associated with the material at the wall.

Our value for the length scale of the less mobile interfacial layer associated with the secondary T_g is in the range of those reported in the literature, which seem to depend on both the glass former and confining medium. For glycerol and

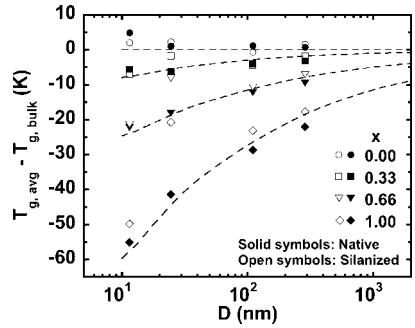

Figure 9. Average glass transition temperature changes from the bulk as a function of pore diameter at different conversions. The dashed lines are intended only as a guide to the eye.

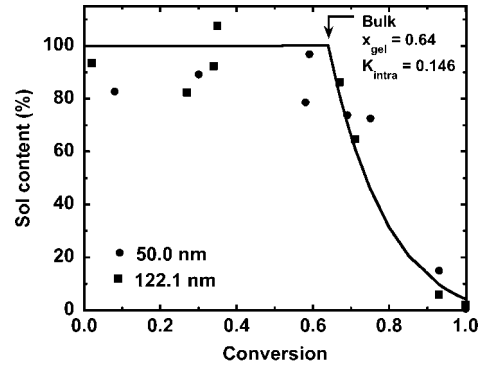

Figure 10. Sol content as a function of conversion for bisphenol M dicyanate ester cured in silanized CPGs with pore diameters of 50.0 and 122.1 nm. The solid line shows the fit to the equation: sol content $(\%) = [((1 - xK_{intra})/(x - 2xK_{intra})) - 1]^2 \times 100$ after gelation, where x is conversion and $K_{intra} = 0.146$ is the probability of intracyclization.

propylene glycol confined in nanoporous glass, the calculated average thickness of the surface layer is small at 0.11 ± 0.06 nm for both the native and silanized systems for pore sizes ranging from 2.5 to 5.0 nm, and the layer thickness is independent of the confining pore size.[9] Longer length scales ranging from 0.96 to 2.5 nm were found for polystyrene/*o*-terphenyl solutions in silanized CPGs for pore diameters from 11.6 to 47.9 nm.[27] Analyses have also been performed using a three-layer model, and in this case, length scales ranging from 0.3 to 0.9 nm have been reported for hydrogen-bonded liquids such as propylene glycol, butylene glycol, and pentylene glycol confined in native CPGs with pore sizes of 2.5−7.5 nm.[39] Although in most cases the length scale is similar to that assumed for cooperatively rearranging regions at T_g, why the glass transition could be observed to occur for a length scale much smaller than the cooperative length scale for some materials is still not clear.

We note that the approach applied to determine the surface layer thickness assumes that the heat capacity change at T_g (per mass of material) for the surface layer and the center do not differ and are the same as the bulk. Although Blum et al. found that the surface may have a different ΔC_p at T_g,[40] the assumption is validated for our system by the same dependence of the total heat capacity change at T_g on conversion independent of confinement size within the error of the measurements, as is shown in Figure 7. It is also found in Figure 7 that the total heat capacities change at T_g decreases with conversion with a more pronounced drop occurring at the gel point, which does not vary upon nanoconfinement (see later).

Influence of Conversion on the Effect of Nanoconfinement on T_g. The effect of nanoconfinement on T_g can be tuned by modification of the molecular structure[10,12] or addition of diluent[11] presumably through the changes in the size of cooperatively rearranging region[10,11] or in chain stiffness.[12] The ability to tune the effect of nanoconfinement on T_g using conversion in the current system is investigated by plotting the change in the glass transition temperature from the bulk as a function of pore diameter at different conversions as shown in Figure 9, using the average T_g as defined in eq 6. The data for both the native and silanized CPGs are shown. The magnitude of the T_g change for the confined system at the same pore size increases with increasing conversion; i.e., the effect of nanoconfinement on T_g is enhanced by curing the resin. The hypothesis that the effect of nanoconfinement on T_g increases with chain stiffness[12] can be readily applied to the BMDC/polycyanurate system since the chain stiffness increases upon polymerization and cross-link formation. Our result can also be explained in terms of the cooperative length scale since the length scale for polycyanurate networks is expected to be larger than bisphenol M dicyanate ester monomer. However, the calculated cooperative length scale based on the Donth's model[23] is 1.57 ± 0.09 nm for fully cured polycyanurate in the bulk state, whereas that for the monomer is larger, at 3.59 ± 0.18 nm. Perhaps this discrepancy is due to the inapplicability of the assumptions made in the Donth's model to our system, namely that (i) the step change in the reciprocal of the specific heat of the glass and the liquid at constant volume ($\Delta(1/C_v)$) is approximated by the isobaric absolute heat capacities at T_g of the glass, C_{pg}, and the liquid, C_{pl}, and (ii) the temperature fluctuation of one average cooperatively rearranging regions (CRR) at temperature T (δT) can be determined using "rules of thumb":[23]

$$\Delta(1/C_v) = \frac{1}{C_{vg}} - \frac{1}{C_{vl}} = 0.74\Delta(1/C_p) \approx 0.74(\Delta C_p/C_{p,av}{}^2)\times \left(1 + \frac{1}{4}(\Delta C_p/C_{p,av}{}^2) + ...\right) \quad (10)$$

$$\delta T = \Delta T/2.5 \quad (11)$$

where ΔC_p is the isobaric heat capacity change at glass transition temperature, $C_{p,av}$ is the average of C_{pg} and C_{pl}, and ΔT is the temperature interval where the $C_p(T)$ curve from DSC varies between 16% and 84% of the ΔC_p step.

Effect of the Intracyclization Side Reaction on T_g Depression of Confined Polycyanurates. In our previous work on bisphenol M dicyanate ester cured in the silanized CPGs, we excluded various factors that could cause the observed T_g depression, such as incomplete cure, negative pressure development due to cure shrinkage, and changes in network structure.[15] In the current study, we further provide experimental evidence that incomplete cure is not the origin of the observations (e.g., see the invariant heat of reaction shown in Table 2). We also showed that the T_g vs conversion and ΔC_p vs conversion relationships were independent of pore size for networks and the same as in the bulk, indicating that the network structure is unchanged under nanoconfinement. To back up this latter claim more substantially, we measured sol content vs conversion for material cured under nanoconfinement. The results are shown in Figure 10. The solid line is the calculated prediction based on our previous modeling of the bulk viscoelastic behavior,[18] in which we concluded that the monomer intracyclization occurs with a probability of 0.146. This model predicts that the gel point occurs at 0.64, in agreement with experimental results for the bulk system.[17] The current experimental sol fraction data for cure under nanoconfinement are also well described assuming the presence of intracyclization with a probability of 0.146 and a gel point of 0.64. Thus, cure under nanoconfinement appears to result in the same degree of intracyclization and the same network structure as cure under bulk conditions, in line

with our conclusions based on the relative average glass transition temperature as a function of conversion (Figure 6) as well as the total heat capacity change at T_g as a function of conversion (Figure 8). Furthermore, monofunctional cyanate ester cured under nanoconfinement, in which the intracyclization side reaction cannot occur, also shows enhanced reactivity and T_g depression, which further corroborates our finding that the T_g depression observed under nanoconfinement is not caused by higher degree of the intracyclization side reaction or by changes in network structure; instead, it is suggested to be caused by an intrinsic size effect.

Conclusions

The cure kinetics and glass transition temperature of bisphenol M dicyanate ester cured in native nanopores were investigated as a function of pore size using differential scanning calorimetry and compared to previous results for silanized pores and to results for the bulk reaction. Nanoconfinement accelerates the cure reaction. In the 11.5 nm native CPG pores, cure is enhanced by a factor of 35 and 43 times, respectively, based on evolution of the primary and secondary T_gs. The enhancement is higher in the native pores than in silanized pores, where accelerations of 20 and 29 are found for T_{g1} and T_{g2} at 11.5 nm. The higher acceleration in the native pores is presumably due to the catalytic effect of the hydroxyl groups on the pore wall surface. In addition, the mechanism suggested in our prior work, in which collision efficiency is enhanced under nanoscale confinement due to the presence of the pore walls, is presumed to be operative.

Two T_gs are observed for both monomer and polycyanurates confined in the native CPGs. The primary T_g is depressed by 60 K at 11.5 nm for the fully cured polycyanurate, and the secondary T_g is 10−33 K above the primary T_g. The length scale associated with the secondary T_g, which is associated with material near the wall, is 0.90 nm, consistent with the cooperative length scale associated with T_g. The magnitude of the effect of nanoconfinement on the T_g depression increases with conversion in our system, presumably due to an increase of chain stiffness on polymerization and cross-link formation and/or changes in the CRR on reaction. The origin of the T_g depression is shown to not be due to incomplete cure or due to changes in network structure; in fact, the latter is argued to be unchanged based on the measurements of T_g, the total heat capacity change at T_g, and the sol content, all as a function of conversion. It is suggested that the origin of the observed depression in T_g is related to an intrinsic size effect.

Acknowledgment. We acknowledge the American Chemical Society Petroleum Research Fund Grant 45416-AC7 for their financial support of this project as well as partial support from the Texas Higher Education Coordinating Board, Advanced Technology Program Grant 003644-0057-2007. We also thank Millipore for their donation of part of the controlled pore glasses. We also thank Yung P. Koh (TTU) for his measurements of nanoconfined benzene as a function of imbibement time.

References and Notes

(1) Alcoutlabi, M.; McKenna, G. B. *J. Phys.: Condens. Matter* **2005**, *17*, R461.
(2) Christenson, H. K. *J. Phys: Condens. Matter* **2001**, *13*, R95.
(3) Fakhraai, Z.; Sharp, J. S.; Forrest, J. A. *J. Polym. Sci., Part B: Polym. Phys.* **2004**, *42*, 4503.
(4) Jackson, C. L.; McKenna, G. B. *J. Non-Cryst. Solids* **1991**, *131*−*133*, 221.
(5) Jackson, C. L.; McKenna, G. B. *Chem. Mater.* **1996**, *8*, 2128.
(6) Park, J.-Y.; McKenna, G. B. *Phys. Rev. B* **2000**, *61*, 6667.
(7) Sharp, J. S.; Teichroeb, J. H.; Forrest, J. A. *Eur. Phys. J. E* **2004**, *15*, 473.
(8) Zhang, J.; Liu, G.; Jonas, J. *J. Phys. Chem.* **1992**, *96*, 3478.
(9) Zheng, W.; Simon, S. L. *J. Chem. Phys.* **2007**, *127*, 194501.
(10) Campbell, C. G.; Vogt, B. D. *Polymer* **2007**, *48*, 7169.
(11) Ellison, C. J.; Ruszkowski, R. L.; Fredin, N. J.; Torkelson, J. M. *Phys. Rev. Lett.* **2004**, *92*, 095702.
(12) Ellison, C. J.; Mundra, M. K.; Torkelson, J. M. *Macromolecules* **2005**, *38*, 1767.
(13) Beiner, M.; Kahle, S.; Abens, S.; Hempel, E.; Horing, S.; Meissner, M.; Donth, E. *Macromolecules* **2001**, *34*, 5927.
(14) Soles, C. L.; Douglas, J. F.; Wu, W.-L.; Peng, H.; Gidley, D. W. *Macromolecules* **2004**, *37*, 2890.
(15) Li, Q. X.; Simon, S. L. *Macromolecules* **2008**, *41*, 1310.
(16) Wang, X.; Zhou, W. *Macromolecules* **2002**, *35*, 6747.
(17) Simon, S. L.; Gillham, J. K. *J. Appl. Polym. Sci.* **1993**, *47*, 461.
(18) Li, Q. X.; Simon, S. L. *Macromolecules* **2007**, *40*, 2246.
(19) Jackson, C. L.; McKenna, G. B. *J. Chem. Phys.* **1990**, *93*, 9002.
(20) Huber, P.; Gruner, S.; Schafer, C.; Knorr, K.; Kityk, A. V. *Eur. Phys. J. Spec. Top.* **2007**, *141*, 101.
(21) Moynihan, C. T.; Easteal, A. J.; DeBolt, M. A.; Tucker, J. *J. Am. Ceram. Soc.* **1976**, *59*, 12.
(22) Badrinarayanan, P.; Zheng, W.; Li, Q. X.; Simon, S. L. *J. Non-Cryst. Solids* **2007**, *353*, 2603.
(23) Hempel, E.; Hempel, G.; Hensel, A.; Schick, C.; Donth, E. *J. Phys. Chem. B* **2000**, *104*, 2460. Donth, E. *J. Polym. Sci., Part B: Polym. Phys.* **1996**, *34*, 2881.
(24) Simon, S. L.; Sobieski, J. W.; Plazek, D. J. *Polymer* **2001**, *42*, 2555.
(25) Nielsen, L. E. *J. Macromol. Sci., Rev. Macromol. Chem.* **1969**, *C3*, 69.
(26) Pascault, J. P.; Williams, R. J. J. *J. Polym. Sci., Part B: Polym. Phys.* **1990**, *28*, 85.
(27) Park, J.-Y.; McKenna, G. B. *Phys. Rev. B* **2000**, *61*, 6667.
(28) Arndt, M.; Stannarius, R.; Gorbatschow, W.; Kremer, F. *Phys. Rev. E* **1996**, *54*, 5377.
(29) Arndt, M.; Stannarius, R.; Groothues, H.; Hempel, E.; Kremer, F. *Phys. Rev. Lett.* **1997**, *79*, 2077.
(30) Barut, G.; Pissis, P.; Pelster, R.; Nimtz, G. *Phys. Rev. Lett.* **1998**, *80*, 3543.
(31) Mel'nichenko, Y. B.; Schüller, J.; Richert, R.; Ewen, B.; Loong, C.-K. *J. Chem. Phys.* **1995**, *103*, 2016.
(32) Patkowski, A.; Ruths, T.; Fischer, E. W. *Phys. Rev. E* **2003**, *67*, 021501.
(33) Pissis, P.; Kyritsis, A.; Barut, G.; Pelster, R.; Nimtz, G. *J. Non-Cryst. Soilds* **1998**, *235*−*237*, 444.
(34) Pissis, P.; Kyritsis, A.; Daoukaki, D.; Barut, G.; Pelster, R.; Nimtz, G. *J. Phys.: Condens. Matter* **1998**, *10*, 6205.
(35) Schönhals, A.; Goering, H.; Schick, C.; Frick, B.; Zorn, R. *Colloid Polym. Sci.* **2004**, *282*, 882.
(36) Schüller, J.; Mel'nichenko, Y. B.; Richert, R.; Fischer, E. W. *Phys. Rev. Lett.* **1994**, *73*, 2224.
(37) Schüller, J.; Richert, R.; Fischer, E. W. *Phys. Rev. B* **1995**, *52*, 15232.
(38) Streck, C.; Mel'nichenko, Y. B.; Richert, R. *Phys. Rev. B* **1996**, *53*, 5341.
(39) Gorbatschow, W.; Arndt, M.; Stannarius, R.; Kremer, F. *Europhys. Lett.* **1996**, *35*, 719.
(40) Blum, F. D.; Young, E. N.; Smith, G.; Sitton, O. C. *Langmuir* **2006**, *22*, 4741.
(41) Simon, S. L.; Gillham, J. K. Unpublished results.

MA802808V